Available online at www.sciencedirect.com
SCIENCE DIRECT®
Coordination Chemistry Reviews 249 (2005) 2631–2641
COORDINATION CHEMISTRY REVIEWS
www.elsevier.com/locate/ccr

Review

Magnetic exchange interactions in perfluorophenyl dithiadiazolyl radicals

Jeremy M. Rawson [a,*], Javier Luzon [b], Fernando Palacio [b]

[a] *Department of Chemistry, The University of Cambridge, Lensfield Road, Cambridge CB2 1EW, UK*
[b] *Instituto de Ciencia de Materiales de Aragon, CSIC-Universidad de Zaragoza, E-50009, Zaragoza, Spain*

Received 19 November 2004; accepted 21 April 2005
Available online 11 July 2005

Contents

Abstract

EPR, electrochemical studies and neutron diffraction studies on a large range of 1,2,3,5-dithiadiazolyl radicals have shown that the spin density distribution is essentially unaffected by substituent effects. The variation of magnetic properties previously reported for a series of perfluorophenyl-dithiadiazolyl radicals *p*-XC_6F_4CNSSN (X = CN, Br, NO_2 and NCC_6F_4) is therefore due to differences in molecular packing. The nearest-neighbour magnetic exchange interactions in these radicals are probed through DFT studies (B3LYP/6-311G**) and are shown to exhibit a variety of both ferromagnetic and antiferromagnetic interactions. All exchange interactions with $|\boldsymbol{J}| > 1\ cm^{-1}$ coincide with close heterocyclic contacts between dithiadiazolyl rings (3.18–4.00 Å) and produce $|\boldsymbol{J}|$ values up to 40 K. An analysis of these interactions indicates that the dominant exchange pathway would appear to be a direct exchange mechanism between radical centres, with orthogonality of the singly-occupied molecular orbitals (SOMOs) favouring ferromagnetic interactions.

Keywords: Dithiadiazolyl; Organic magnet; DFT; Magnetostructural correlation

* Corresponding author. Tel.: +44 1223 336319; fax: +44 1223 336362.
E-mail addresses: jmr31@cus.cam.ac.uk (J.M. Rawson), palacio@posta.unizar.es (F. Palacio).

0010-8545/$ – see front matter © 2005 Elsevier B.V. All rights reserved.
doi:10.1016/j.ccr.2005.04.020

1. Introduction

The magnetic behaviour of organic radicals has been the subject of considerable academic interest for many years and has seen a renaissance with the discovery of the first organic molecular magnets such as **1**–**3** in the last 20 years [1]. The design of organic ferromagnets is conceptually very simple but is extremely complex in its execution [2]. It merely requires the crystallisation of radicals in the solid state in such a way that the dominant exchange interaction between radicals is ferromagnetic and propagates throughout the lattice in three dimensions. This simple statement belies a number of immense theoretical and experimental difficulties. For example, open shell organic molecules are often extremely reactive and need to be stabilised via π-delocalisation and/or inclusion of bulky substituents to provide both thermodynamic and kinetic stability. In addition the dominant magnetic interaction between radicals must be ferromagnetic. The theory of exchange interactions in transition-metal based systems were developed in the 1950s by Andersen in terms of direct exchange, superexchange and double-exchange mechanisms [3]. Our understanding of the superexchange mechanism was further expanded by Goodenough and Kanamori [4]. In comparison, a coherent view of the through-space exchange mechanisms operative between organic radicals has not been well understood. Amongst a number of models which have been put forward, one of the most popular approaches to rationalise the intermolecular exchange interaction between organic radicals is that proposed by McConnell [5]. The McConnell I mechanism proposed that *the matching of regions of positive and negative spin densities on neighbouring molecules* (*associated in a π-stacked 'pancaked' structure*) *will lead to a ferromagnetic interaction*. Conversely the matching of regions with the same sign of the spin density should lead to an antiferromagnetic interaction.

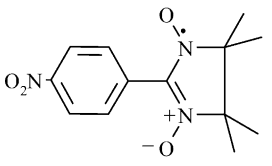

1

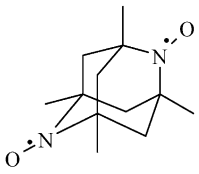

2

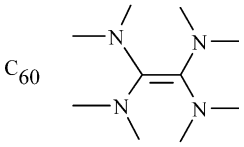

3

Some elegant studies on cyclophane derivatives by Iwamura *inter alia* supported this mechanism [6], but this exchange mechanism has recently come under scrutiny. A statistical analysis of a large number of nitronyl nitroxide radicals (such as **1**) by Novoa and Deumal indicated that there appears to be no correlation between the intermolecular contacts and the sign or strength of the exchange interaction [7]. One of the key problems with the McConnell I model is that it is based upon contacts between regions of positive and negative spin density on different molecules, yet in many cases there are few short intermolecular contacts between regions of positive (or negative) spin density. Certainly in the case of nitronyl nitroxides studied by Novoa and Deumal [7], the closest of the intermolecular N···O or O···O contacts all lie beyond the sum of the van der Waals radii of N and O (3.2 Å). Moreover the majority of intermolecular contacts are not between π-stacked radicals (as suggested by McConnell). Nor did McConnell consider the more general case of angular dependence between π-radicals. Further theoretical studies by Novoa indicated that the nature of the substituent group on the nitronyl nitroxide, despite formally bearing very little unpaired spin density, plays an important role in determining both the sign and strength of the exchange pathway [7].

In the absence of any rigorous models for analyzing/predicting the magnetic behaviour of radicals, it is impossible to develop new organic magnets in a systematic manner. The task is made yet more demanding since the relative disposition of the spin density distributions on neighbouring molecules is dependent not only on the electronic effects of the substituent(s) but also on the nature of the intermolecular interactions. Whilst an increasing number of supramolecular synthons are now available [8] to provide some control on the nature of intermolecular contacts, these contacts are by no means infallible (see for example interactions between carboxylic acid groups [9]) and structure prediction for neutral organics is a research area which is still very much in its infancy [10].

In recent years we have undertaken a series of magnetic studies on a group of stable five-membered heterocyclic thiazyl radicals [11]. Here we focus on a closely-related group of dithiadiazolyl radicals **4**–**7** and compare and contrast their magnetic properties to those of the larger and more extensively studied group of nitronyl nitroxides. In nitronyl nitroxides the positive spin density is localised on the N and O atoms. However close contacts between these regions of positive spin density is disfavoured due to the electrostatically repulsive nature of the $O^{\delta-}\cdots O^{\delta-}$ contacts coupled with the steric protection of the N atom. In contrast the lack of steric protecting groups coupled with the polarity of the S–N bond often favours intermolecular $S^{\delta+}\cdots N^{\delta-}$ contacts close to or less than the sum of the van der Waals radii [12]. Here we show that the exchange interaction between these thiazyl radicals can be predominantly attributed to a direct exchange process in which the sign of the exchange interaction can be determined on the basis of simple orbital orthogonality rules.

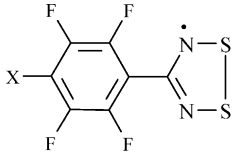

4 X = CN
5 X = Br
6 X = O_2N
7 X = NCC_6F_4

2. Results

Density functional theory (DFT) is a semi-empirical approach and does not explicitly deal with electron-correlation which is expected to play a vital role in determining singlet–triplet gaps [13]. Nevertheless in recent years DFT has proved to be an extremely powerful approach to the determination of the exchange interaction in both metal clusters [14] and through space interactions in organic radicals. Indeed systematic studies by Novoa and Yamaguchi have shown that the bulk magnetic behaviour of organic solids can be determined by a determination of the local nearest-neighbour exchange interactions between radicals [7]. In particular Novoa's studies on aryl-substituted nitronyl nitroxide radicals clearly showed that the phenyl substituent, which itself bore negligible spin density, contributed significantly to the magnetic exchange pathway [7].

The general approach to determine the magnetic exchange interaction between two nearest neighbour radicals is to compute the energies of the triplet (E_T) and broken symmetry singlet (E_{BS}) states. The broken symmetry singlet state is a DFT state composed of pure magnetic states in which all the α-magnetic orbitals are located on one magnetic center and all the β-magnetic orbitals are located on the other magnetic center [15].

Within the context of the Hamiltonian $H = -2\boldsymbol{J}S_1 \cdot S_2$ where $\boldsymbol{J}$ is the exchange interaction between spins S_1 and S_2, the energy between the singlet and triplet is denoted by $2\boldsymbol{J}$. Yamaguchi proposed [16] that the exchange interaction could be estimated from the energies of the broken symmetry singlet and triplet states and their expectation values $\langle S^2 \rangle$, according to the expression:

$$\boldsymbol{J} = -\frac{E_{HS} - E_{BS}}{\langle S^2 \rangle_{HS} - \langle S^2 \rangle_{BS}}$$

In the following sections we describe the geometry of all the nearest neighbour interactions within the structures of **4α**, **4β**, **5** and **6** which lead to significant values of $|\boldsymbol{J}|$. Density functional calculations were carried out using the hybrid exchange-correlation functional B3LYP which has proved to correct the tendency of the local and GGA exchange correlation functionals to overestimate the stability of the singlet state (with respect to the triplet) [17]. Two different basis sets were employed; the polarised split-valence double-zeta (6-31G**) and triple-zeta (6-311G**) Pople basis sets in order to test the convergence of the calculation with the size of the basis set. All calculations exhibited very good agreement between the two different basis sets. Where larger discrepancies ($\pm 2\,cm^{-1}$) were apparent there was no doubt as to both the sign and relative magnitudes of these interactions. As a consequence it was not considered necessary to include more diffuse functions in the basis set. Values of $|\boldsymbol{J}|$ were considered significant when $|\boldsymbol{J}| > 1\,cm^{-1}$.

We begin with a study of **4β** and **6**. Both these radials exhibit bulk magnetic order. Whilst the dominant exchange interaction in **4β** is antiferromagnetic, it is ferromagnetic in **6**. We then extend this approach to **4α** and **5** in order to rationalize the lack of long-range magnetic order in these two derivatives. We will then apply the results derived from the analysis of **4**–**6** to the recently prepared derivative **7**.

2.1. Exchange interactions in β-p-NCC$_6$F$_4$CNSSN

The dithiadiazolyl radical β-*p*-NCC$_6$F$_4$CNSSN, **4β**, is one of the most extensively studied organic molecular magnets. It was originally reported to order as a canted antiferromagnet at 36 K [18]. The magnetic phase transition has been investigated by an armoury of ac and dc susceptibility experiments as well as heat capacity studies [19]. Additional powder neutron diffraction [19], μ-SR and single crystal EPR studies [20] have been utilised to investigate the magnetic structure. Further studies have indicated that the application of pressure can raise the ordering temperature of this material to values in excess of 65 K [21]. The crystal structure of **4β** exhibits a chain-like motif in which molecules are linked via electrostatic $CN^{\delta-}\cdots S^{\delta+}$ interactions along the crystallographic *c*-axis [18]. The structure of **4β** is polar (orthorhombic *Fdd2*) and it is the acentric nature of the crystal structure which lends itself to a non-colinear spin arrangement in the ordered phase. The high symmetry of the orthorhombic structure with half a molecule in the asymmetric unit favours a small number of chemically distinct intermolecular contacts. The calculated exchange interactions to all chemically different nearest neighbour molecules were determined under the broken symmetry approach. Only one of the intermolecular contacts leads to a significant exchange coupling (>1 cm^{-1}) (Table 1). This exchange interaction is associated with a short S···N contact of 3.488 Å. Each molecule forms four symmetry equivalent interactions ($\boldsymbol{J}_1$) of this type forming a distorted tetrahedral geometry (Fig. 1). Propagation of this interaction throughout the lattice leads to a three-dimensional diamond-like exchange pathway [22].

It is noteworthy that the closest intermolecular contact ($CN^{\delta-}\cdots S^{\delta+}$) appears to be a structure-directing motif and is observed elsewhere, e.g. in **4α** [23] and **7** [24] as well as in other non-fluorinated derivatives such as NCCNSSN [25], *m*-NCC$_6$H$_4$CNSSN and *p*-NCC$_6$H$_4$CNSSN [26]. Yet the magnetic exchange interaction ($\boldsymbol{J}_2$) associated with this structure-directing interaction can be considered negligible at ca. $10^{-2}\,cm^{-1}$. This value is in good agreement with experimental measurements on *p*-NCC$_6$H$_4$CNSSN·PHTP (PHTP = perhydrotriphenylene) [22]. In this host-guest complex molecular chains of *p*-NCC$_6$H$_4$CNSSN radicals are

Table 1
Closest contacts between neighbouring molecules in β-*p*-NCC$_6$F$_4$CNSSN and the corresponding calculated Broken-Symmetry DFT coupling constants

Pathway	Contact	*d* (Å)	$\boldsymbol{J}$ (cm^{-1}) (6-31G**)	$\boldsymbol{J}$ (cm^{-1}) (6-311G**)
$\boldsymbol{J}_1$	S···N	3.488	−32.58	−31.38
$\boldsymbol{J}_2$	CN···S	2.986	−0.03	−0.04

Exchange interactions are based upon the crystal data at 160 K.

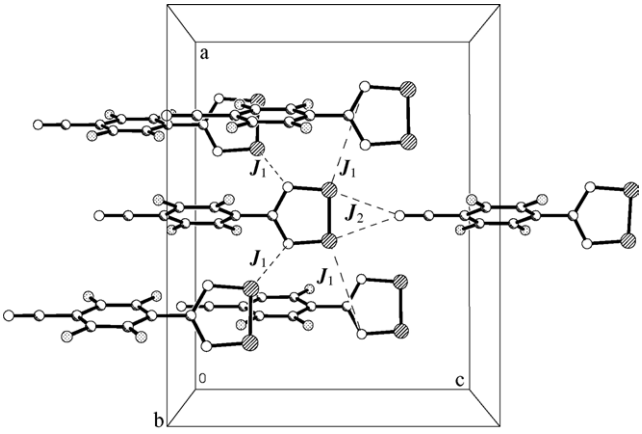

Fig. 1. Crystal structure of β-*p*-NCC_6F_4CNSSN with exchange pathways labelled. Intermolecular contacts and calculated exchange couplings are presented in Table 1. (Structural data taken from reference [18]).

linked via CN···S interactions but are magnetically insulated from other chains by the PHTP host lattice. Magnetic measurements indicate that this complex is a near perfect paramagnet, exhibiting Curie behaviour down to the lowest recorded experimental temperatures (1.8 K) [22], consistent with the very small calculated value of $\boldsymbol{J}_2$.

The Weiss constant (θ) within the Curie–Weiss Law (Eq. (1)) can be related to the individual exchange interactions via the Mean Field approach (Eq. (2)):

$$\chi = \frac{Ng^2\beta^2}{3k(T-\theta)}S(S+1) \tag{1}$$

$$\theta = \frac{z\boldsymbol{J}S(S+1)}{3k} \tag{2}$$

where z is the number of nearest neighbours. Alternatively we might consider a more analytical expression where a sum of all $\boldsymbol{J}$ terms is included rather than z times the average exchange term (Eq. (3)):

$$\theta = S(S+1)\frac{\sum \boldsymbol{J}_i}{3k} \tag{3}$$

Within the mean field approach, the magnitude of θ is expected to give an upper limit to the magnetic ordering temperature. Suppression of the ordering temperature may occur due to magnetic frustration [27], i.e. competing sets of interactions within the system which preclude ordering, or because of the low dimensionality of the exchange pathway. For Heisenberg spins (such as organic radicals) bulk order will only occur for exchange pathways which extend in three dimensions. The ordering temperature is then dependent on the weakest of the interactions necessary to propagate the exchange in three dimensions [28].

In the case of **4β** the magnetic ordering temperature (36 K) is in good agreement with that predicted from the calculated values based on mean field theory, $\theta = -45$ K.

2.2. Exchange interactions in *p*-$O_2NC_6F_4CNSSN$

Radical **6** has been shown to be a rare example of a bulk organic ferromagnet with a Curie temperature of 1.3 K under ambient pressure [29]. Calorimetry studies have recently shown that an increase in pressure raises the ordering temperature up to 1.8 K under 11.6 kbar [30]. The structure of **6** is polar (tetragonal, space group $P4_12_12$) [29]. Like **4β** the molecule sits on a two-fold rotation axis. In this case the molecules pack together to form molecular chains via electrostatic $NO_2\cdots S$ contacts (3.186 and 3.323 Å) comparable to the CN···S interactions in both **4α** and **4β** (Fig. 2a). In **4α** these chains are related by an inversion center and align antiparallel [23]. In **4β** they are related via a diamond glide and align coparallel [18]. In **6** the chains are related via a 4_1 screw axis along the crystallographic *c*-axis. The four-fold symmetry combined with the molecule lying on a two-fold rotation axis generates four equivalent contacts to other radicals; two in the plane above and two below (Fig. 2b). The shortest of these contacts is a heterocyclic S···N of 3.658 Å [29]. A theoretical analysis of the exchange interactions indicates that the strongest exchange coupling is via this S···N contact and is weakly ferromagnetic ($\boldsymbol{J}_1 = +1.14\,cm^{-1}$). All other interactions including those formed via the close, structure-directing, $NO_2\cdots S$ contact ($\boldsymbol{J}_2 = -0.03\,cm^{-1}$) are more than an order of magnitude smaller. A simple analysis of these interactions predict Weiss constants of +1.80 K and +1.64 K for the 6-31G** and 6-311G** basis sets, respectively. Within the mean-field approximation, this leads to an upper limit for the magnetic ordering temperature of 1.80–1.64 K, in excellent agreement with the observed value [29] of 1.3 K.

2.3. Exchange interactions in α-*p*-NCC_6F_4CNSSN

The α-phase of *p*-NCC_6F_4CNSSN (**4α**) was the first reported dithiadiazolyl radical to retain its monomeric nature in the solid state [23]. Preliminary magnetic measurements on a Faraday Balance exhibit a broad maximum in χ around 8 K indicative of short-range antiferromagnetic interactions [23]. However comparable studies on the β-phase of *p*-NCC_6F_4CNSSN on the same equipment [31] yielded an ordering temperature of 38 K (ca. 2 K higher than the value determined by a number of independent measurements [19,20] by SQUID, heat capacity studies, μ-SR, single crystal EPR and powder neutron diffraction). The resultant uncertainty in the temperature measurements for **4α** mean that the exact position of the maximum in χ precludes some detailed

Table 2
Closest contacts between neighbouring molecules in *p*-$O_2NC_6F_4CNSSN$ and the corresponding calculated Broken-Symmetry DFT coupling constants, based on the crystal structure geometry determined at 160 K

Pathway	Contact	*d* (Å)	$\boldsymbol{J}$ (cm^{-1}) (6-31G**)	$\boldsymbol{J}$ (cm^{-1}) (6-311G**)
$\boldsymbol{J}_1$	S···N	3.658	+1.26	+1.15
$\boldsymbol{J}_2$	$NO_2\cdots S$	3.186, 3.323	−0.03	−0.04

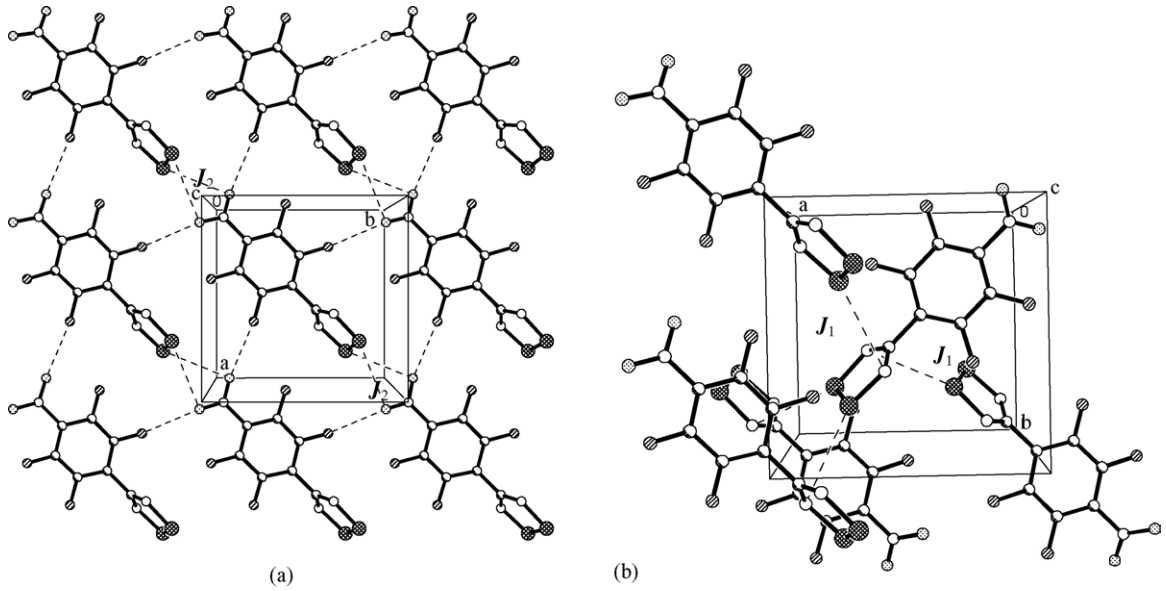

Fig. 2. Crystal structure of *p*-$O_2NC_6F_4CNSSN$ illustrating (a) the intermolecular contacts in the *ab* plane and (b) the inter-plane S···N contacts of which two of the four $\boldsymbol{J}_1$ contacts are labelled. Intermolecular contacts and calculated exchange couplings are presented in Table 2. (Structural data taken from reference [29].)

discussion of the magnetic behaviour at this time, although it is likely to occur below 10 K. In addition formation of the thermodynamically preferred phase **4β** has persistently hampered further attempts to isolate and undertake more systematic studies on **4α**.

The structure of **4α** is triclinic (space group *P*-1) with a single molecule in the asymmetric unit [23]. The low symmetry of the triclinic crystal system leads to a more varied range of close intermolecular contacts. The shortest of these are $CN^{\delta-}\cdots S^{\delta+}$ interactions which link radicals together into molecular chains ($d_{CN\cdots S} = 3.068$ and 3.105 Å). An additional web of S···S contacts links chains in an antiparallel fashion in the *ab* plane ($d_1 = 3.601$, $d_2 = 3.668$ Å). Along the *c*-axis a pair of close-heterocyclic S···N contacts ($d_{S\cdots N} = 4.186$ and 4.269 Å) form a centrosymmetric dimer analogous to *p*-IC_6H_4CNSSN [32] but with substantially larger intermolecular separation (4.186 and 4.269Å, cf. S···N in *p*-IC_6H_4CNSSN at 3.116 and 3.152 Å). These loosely associated dimers of **4α** are linked via N···N contacts (5.064 Å) about a crystallographic inversion centre. These nearest neighbour intermolecular interactions are depicted in Fig. 3.

Unlike both **4β** and **6** in which there is a single dominant exchange interaction, an analysis of all nearest-neighbour exchange interactions in **4α** reveals two significant interactions (Table 3). Both these interactions are propagated via close intermolecular heterocyclic contacts and comprise competing antiferromagnetic ($\boldsymbol{J}_1$) and ferromagnetic ($\boldsymbol{J}_2$) interactions of similar magnitude. Notably the shorter of the two intermolecular S···S contacts ($\boldsymbol{J}_3$) in the *ab* plane (Fig. 3a) propagates a negligibly small exchange coupling, whereas the longer propagates an antiferromagnetic interaction ($\boldsymbol{J}_1 \sim -7\,cm^{-1}$). The second significant exchange

Table 3
Closest contacts between neighbouring molecules in α-*p*-NCC_6F_4CNSSN and the corresponding calculated Broken-Symmetry DFT coupling constants

Pathway	Contact	*d* (Å)	$\boldsymbol{J}$ (cm^{-1}) (6-31G**)	$\boldsymbol{J}$ (cm^{-1}) (6-311G**)
$\boldsymbol{J}_1$	S···S	3.668	−6.02	−8.80
$\boldsymbol{J}_2$	S···N	4.186	+9.15	+7.58
	S···N	4.269		

interaction ($\boldsymbol{J}_2$) is of a similar magnitude to $\boldsymbol{J}_1$, but of opposite sign and links molecules along the *c*-axis. The propagation of these two interactions ($\boldsymbol{J}_1$ and $\boldsymbol{J}_2$) throughout the crystal lattice generates a one-dimensional magnetic chain structure with alternating ferromagnetic and antiferromagnetic interactions. The data presented in Table 3 indicate that the determination of the exchange interaction has not fully converged at the 6-311G** level. As a consequence there is some uncertainty in which parameter is likely to dominate the magnetic behaviour in this instance. Nevertheless, the opposing nature of the signs of these two dominant interactions lead us to predict upper limits for the short-range ordering of a few Kelvin, somewhat less than the experimental value (ca. 8 K). This inconsistency is slightly at odds with the excellent agreement evaluated for **4β** and **6**, and merits further experimental studies. Despite this, the lack of long-range magnetic order present in **4α** is merely a reflection of the one-dimensional nature of the exchange pathway.

2.4. Exchange interactions in *p*-BrC_6F_4CNSSN

This radical also crystallizes in a polar space group (orthorhombic *Aba2*) [33]. Here molecules are linked via short S···N contacts (3.175 Å) along the crystallographic

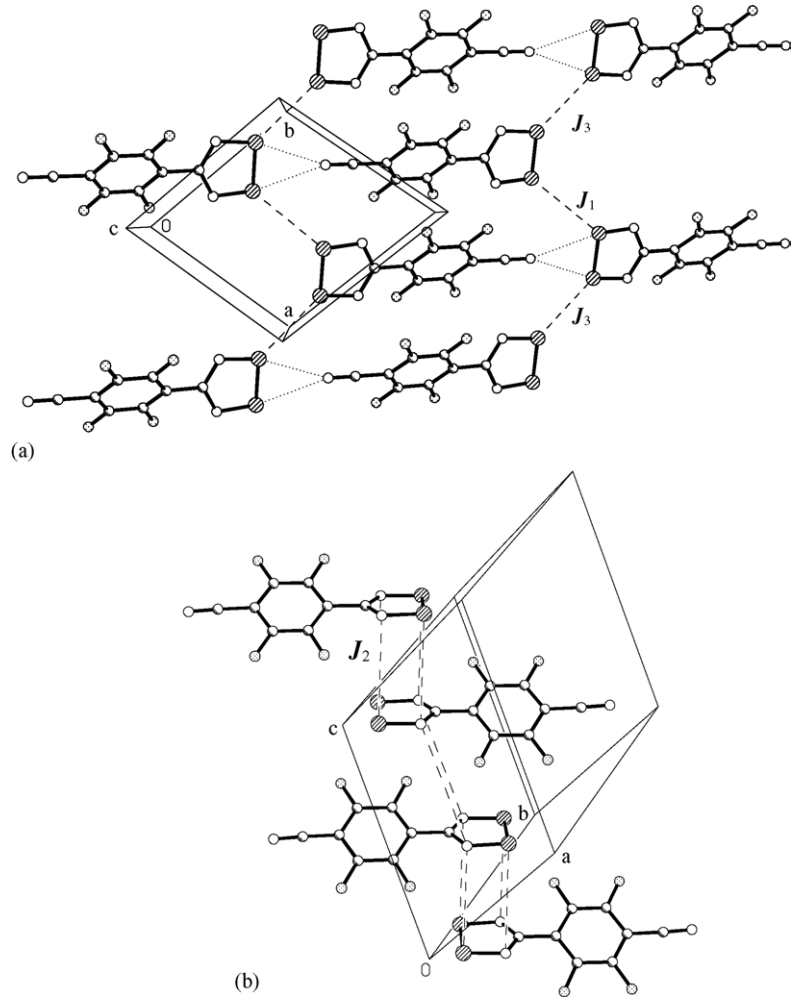

Fig. 3. Crystal structure of α-*p*-NCC_6F_4CNSSN with exchange pathways labelled. Intermolecular contacts and calculated exchange couplings are presented in Table 1. (Structural data taken from reference [23].)

c-axis (Fig. 4a). In addition the radicals form a π-stacked motif parallel to the crystallographic *a*-axis with intermolecular S···N and S···S contacts in the range 3.675–3.999 Å (cf. sum of van der Waals radii perpendicular to the ring plane at 3.2 and 4.0Å for S···N and S···S, respectively). The magnetic behaviour of *p*-BrC_6F_4CNSSN is characterised by Curie–Weiss behaviour ($\theta = -27$ K) in the high temperature regime but does not exhibit either the λ-type peak or broad maximum above 1.8 K associated with either long range or short-range antiferromagnetic order [33].

Table 4
Closest contacts between neighbouring molecules in *p*-BrC_6F_4CNSSN and the corresponding calculated Broken-Symmetry DFT coupling constants

Pathway	Contact	*d* (Å)	$\boldsymbol{J}$ (cm^{-1}) (6-31G**)	$\boldsymbol{J}$ (cm^{-1}) (6-311G**)
$\boldsymbol{J}_1$	N(1)···S(1a)	3.634		
	N(1)···S(2a)	4.182		
	S(1)···S(1a)	3.865	−9.86	−7.62
	S(2)···C(1a)	4.196		
	N(2)···N(2a)	4.377		
$\boldsymbol{J}_2$	S(2)···S(2a)	3.675		
	S(2)···N(2a)	3.738	+8.51	+7.52
	S(2)···S(1a)	4.371		
$\boldsymbol{J}_3$	S···N	3.175	−8.38	−8.25

Exchange interactions are based upon the crystal data at 160 K.

Amongst all the nearest neighbour interactions, three significant exchange interactions were found. $\boldsymbol{J}_1$ and $\boldsymbol{J}_2$ link molecules along the *a*-axis and alternate in sign whilst $\boldsymbol{J}_3$, which links molecules in the *c*-direction, is antiferromagnetic.

The magnetic motif generated by these three interactions is a two-dimensional grid in which each molecule forms three antiferromagnetic ($\boldsymbol{J}_1$ and two $\boldsymbol{J}_3$) and one ferromagnetic ($\boldsymbol{J}_2$) interaction. Within the mean-field approximation, these interactions lead to an expected Weiss constant of −26 K (6-31G**) or −24 K (6-311G*) in excellent agreement with the experimental value ($\theta = -27$ K) [33]. The absence of long range magnetic order can be directly attributed to the combined effects of the very small spin anisotropy associated with unpaired electrons in π-type orbitals, coupled with the two dimensional nature of the exchange pathway (Fig. 5).

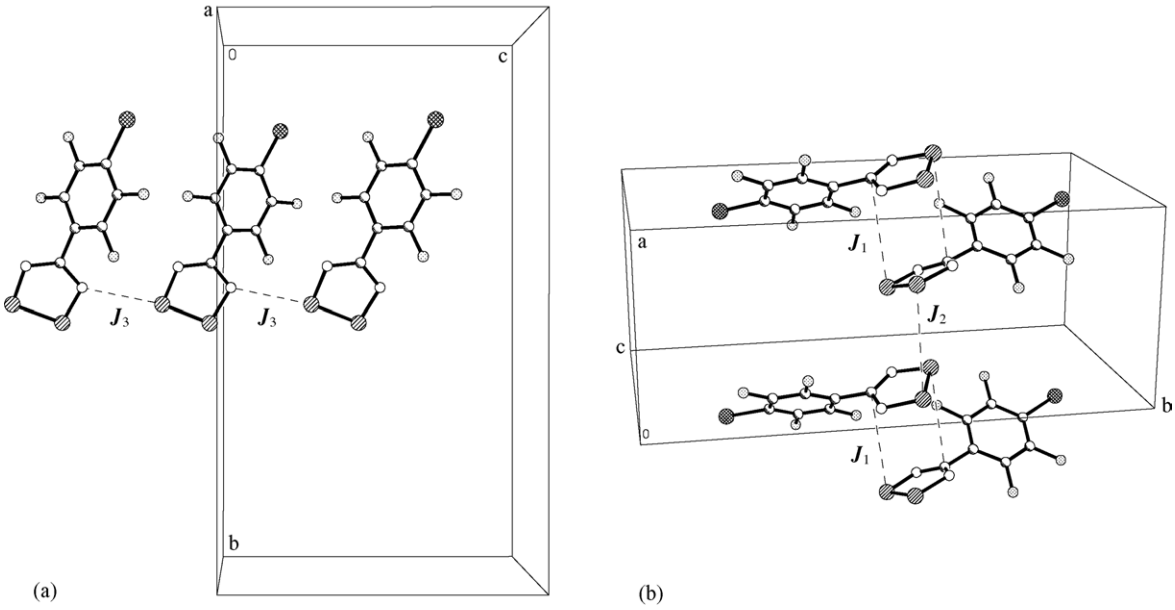

Fig. 4. Crystal structure of *p*-BrC_6F_4CNSSN with exchange pathways labelled. Intermolecular contacts and calculated exchange couplings are presented in Table 4. (Structural data taken from reference [33].)

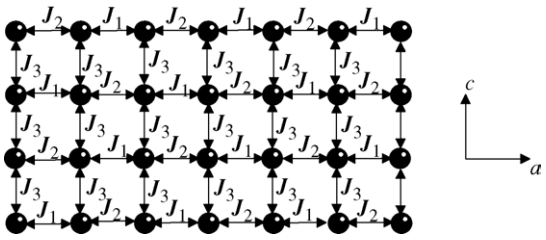

Fig. 5. Exchange pathway in *p*-BrC_6F_4CNSSN, with relative orientations of the crystallographic axes.

Moreover the nature of the exchange pathways induces frustration into the system which may also suppress any short-range ordering.

3. Discussion

3.1. Spin density distribution in dithiadiazolyl radicals

A number of theoretical calculations have shown [34] that the unpaired spin density is almost entirely localised on the heterocyclic S/N ring with a small negative spin density on the heterocyclic C atom. The functional group attached to this C appears to have only a very small effect on the electronic properties of the heterocyclic ring, e.g. redox behaviour [35] and EPR spectra [34,36]. A detailed analysis of the isotropic and anisotropic hyperfine interactions in the EPR spectra provides [34,37] quantitative estimates of the spin density distribution (s and π electron densities) at N which are in excellent agreement with DFT calculations. However they give no direct information on the spin density distribution at either C or S (both of which have very low natural abundances of spin active isotopes). More recently we have undertaken polarised neutron diffraction studies [38] on **6** which have confirmed the spin density distribution at N and also allowed a direct observation of the residual π-spin density at S predicted by DFT studies. The spin density distribution for **6** is shown in Fig. 6. Spin polarisation within the unrestricted Hartree-Fock (UHF) formalism may leads to a slight excess of ('spin-up') α-spin. This excess is compensated by a small negative spin density ('spin-down') β-spin elsewhere in the molecule. The spin polarisation approach leads to a build up of negative spin density at regions in the molecule which would be considered

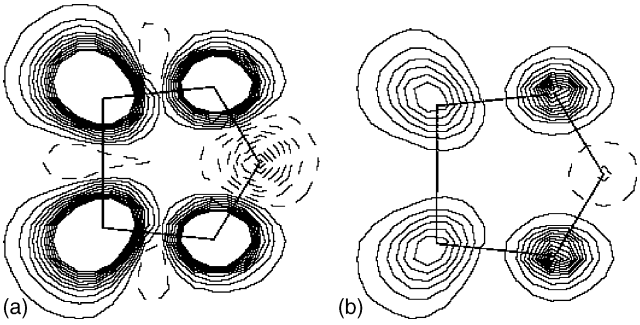

Fig. 6. Spin density distribution around the dithiadiazolyl ring in **6** from polarised neutron diffraction experiments projected onto the heterocyclic plane using a multipolar expansion approach. Solid lines represent regions of positive spin density, dashed lines represent regions of negative spin density; (a) low levels $5 \pm n(10) m\mu_B$ Å^{-2}; (b) high levels $25 \pm n(50) m\mu_B$ Å^{-2}. The spin populations determined from a multipolar expansion model of the experimental density are: S +0.28, N +0.25, C −0.06 (see reference [38]).

to be formally nodal within a restricted Hartree–Fock (RHF) approach. In the case of **6**, negative spin density is located at the heterocyclic C atom and in the heterocyclic ring plane.

For the majority of dithiadiazolyl radicals, two molecules associate via a π^*–π^* bonding interaction between coplanar rings [36]. This leads to a rather weak π^*–π^* bond, not dissimilar to that described [39] by Miller in certain $TCNE^{\bullet-}$ salts. The a_2 symmetry of the SOMO provides a number of symmetry-allowed bonding conformations of which the *cis*-cofacial arrangement is most prevalent but by no means unique. Solution EPR studies have allowed the dimerisation energy to be estimated at ca. 35 kJ mol^{-1} for a number of derivatives [40]. In the case of **4**–**6** this dimerisation is suppressed through the introduction of perfluoroaryl substituents (which increase the steric bulk of the substituent making dimerisation less favourable) and the introduction of electropositive and/or electronegative groups. The latter provide an enhanced ionic contribution to the lattice energy such that the favourable ΔH_{dim} contribution becomes less significant in relation to ΔH_{latt}. This complex combination of steric and electronic effects, inhibits π^*–π^* dimerisation yet still accommodates close heterocyclic contacts. These are either electrostatically favourable $S^{\delta+}\cdots N^{\delta-}$ or van der Waals S···S contacts between polarisable S atoms. In order to understand the nature of the intermolecular magnetic exchange interaction we focus on the SOMO–SOMO interaction associated with the local ferromagnetic and antiferromagnetic interactions identified between dithiadiazolyl radical pairs within the structures of **4**–**6**.

3.2. Ferromagnetic interactions between dithiadiazolyl radicals

In the case of both **4α** and **5**, 'cofacial' π^*–π^* interactions are both strongly ferromagnetic ($J_3 = +7.58$ cm^{-1} and $J_2 = +7.52$ cm^{-1} for **4α** and **5**, respectively). In both cases the two rings adopt formally non-bonding geometries in which the overlap regions coincide with the nodal planes of the SOMOs, i.e. the two magnetic orbitals are mutually orthogonal (Fig. 7a and b). In the case of **6** the two orbitals are again mutually orthogonal. In this case the two radicals do not interact via a coplanar π^*–π^* interaction. Instead the orbital orthogonality arises from twisting of the two ring planes so that they are almost mutually perpendicular.

The mutually orthogonal, non-bonding nature of the SOMOs favours ferromagnetic coupling in the same way that mutually orthogonal d-orbitals on a transition metal ion (or orthogonal magnetic orbitals in a dimeric metal complex) favour coparallel spin alignment. This approach is not inconsistent with the McConnell model. Within the context of the McConnell mechanism, a ferromagnetic interaction occurs when regions of positive and negative spin density overlap. Since these regions of negative spin density occur at nodal planes then any intermolecular geometries which favour coincident overlap of a nodal plane (within the RHF approximation) with a region of unpaired (positive) spin density should stabilize a ferromagnetic interaction. The corollary is that the McConnell mechanism is merely a reflection of orbital orthogonality principles evolved elsewhere. Some

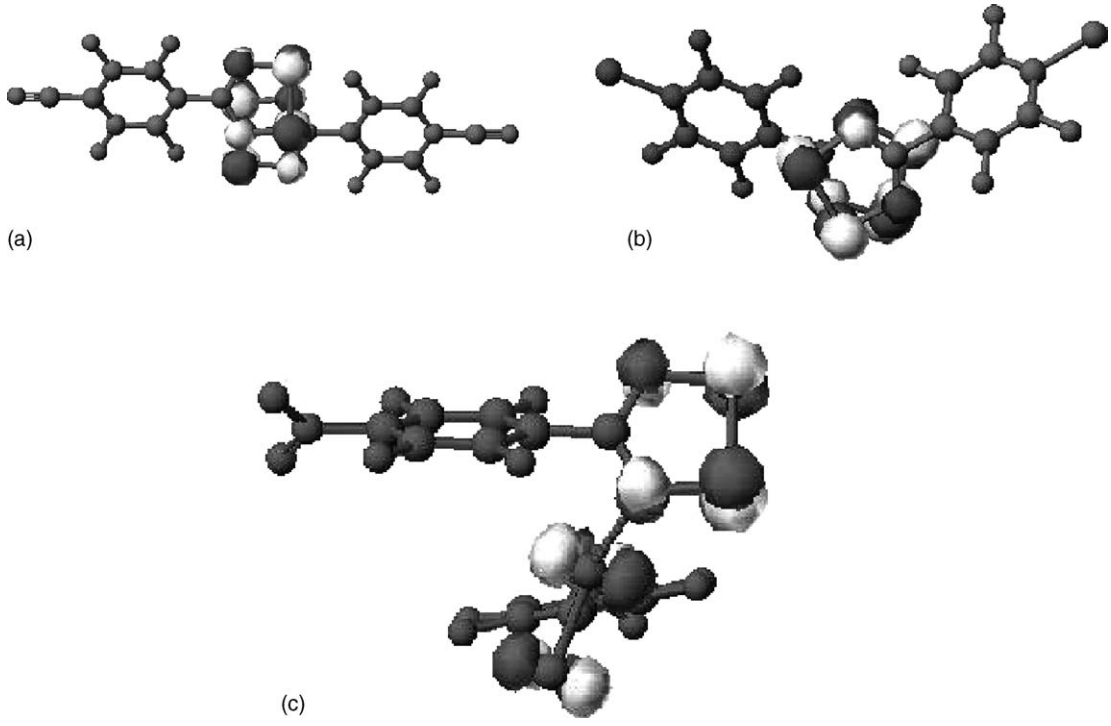

Fig. 7. Orthogonal nature of the SOMO–SOMO interactions in (a) **4α**; (b) **5**; (c) **6**.

consideration of the orbital orientation must be considered and was not expanded upon by McConnell who considered only a π–π interaction between coplanar π-systems. Radical **6** provides an excellent example in this respect. Here the S···N contact depicted in Fig. 7c is clearly between regions of positive spin density at S and N. According to McConnell this would be expected to favour an antiferromagnetic interaction if orientation effects are ignored. Yet the relative orientation of these two rings makes them mutually orthogonal and a ferromagnetic interaction results.

3.3. Antiferromagnetic interactions between dithiadiazolyl radicals

In the case of **4α**, a π^*–π^* interaction between coplanar rings via overlap of an 'edge' of each heterocyclic ring produces a weak bonding interaction which stabilizes an antiferromagnetic ground state (Fig. 8a). In the case of **4β** a single out-of-plane π^*–π^* S···N contact also generates a bonding interaction which favours an antiferromagnetic interaction (Fig. 8b). In **5** there are two antiferromagnetic interactions; one is via a π^*–π^* interaction between coplanar rings with a net bonding interaction at the S atoms whereas the second interaction can be considered as a π^*–π^* bonding interaction close to the ring plane (Fig. 8c and d).

Any weak π^*–π^* bonding interaction between radicals is expected to stabilise the open shell singlet state (although it should be noted that substantial orbital overlap will, of course, lead to a π^*–π^* closed shell ground state).

3.4. A comparison of exchange interactions in dithiadiazolyls and nitronyl nitroxides

This simple SOMO–SOMO analysis initially seems at odds with the detailed studies reported for the nitronyl nitroxide radicals [7]. In that case there appeared to be no direct correlation between the nature of the exchange interaction and the intermolecular geometry. However the difference between the two radical systems can be attributed to the nature of the exchange pathway. In the case of the nitronyl nitroxides, the O···O (as well as N···O and N···N) contacts are almost invariably beyond the sum of the van der Waals radii (3.2 Å), i.e. the minimum distance between two atoms which may be considered to be non-bonding. Whilst the van der Waals radius of N can be considered spherical (1.60 Å), a statistical analysis of S···S contacts in the Cambridge Crystallographic database showed [41] that the softer, more polarisable S atom exhibits substantial anisotropy with a minor radius close to the ring plane of 1.60 Å and a radius perpendicular to the ring plane of 2.0 Å. As a consequence we consider both S···N and S···S contacts close to the ring plane to be significant when they are less than 3.2 Å. In contrast the sum of the van der Waals radii for S···N and S···S contacts perpendicular to the ring plane are 3.6 and 4.0 Å, respectively.

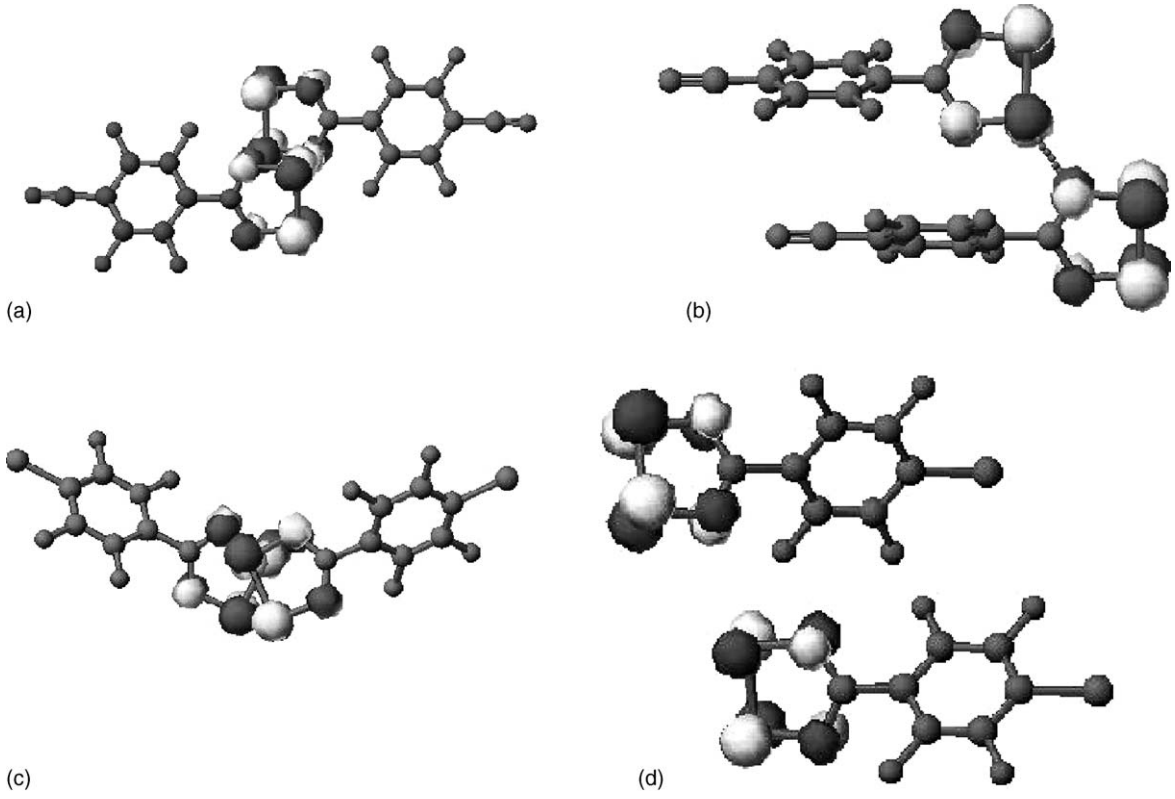

Fig. 8. SOMO–SOMO interaction emphasizing the bonding character (a) via two out-of-plane S···N contacts in **4α**; (b) via a single out-of-plane S···N contact in **4β**; (c) via an out-of-plane S···S contact in **5**; (d) via a single in-plane contact S···N contact in **5**.

The majority of the significant exchange pathways identified in **4**, **5** and **6** exhibit close contacts within this range. Moreover they are favoured electrostatically ($S^{\delta+}\cdots N^{\delta-}$) or via dispersion forces (S···S) whereas the $O^{\delta-}\cdots O^{\delta-}$ contact is electrostatically disfavoured in nitronyl nitroxides [42]. Close contacts to the nitroxide N atom are inhibited by steric factors and the resultant intermolecular contacts are usually N–O···H–C. Additional DFT studies on these nitronyl nitroxide radicals indicate that the substituent plays a key role in determining both the strength and sign of the magnetic exchange pathways [7].

3.5. Extension towards novel dithiadiazolyl and related radicals

In the case of dithiadiazolyl radical **7**, some structural control of the crystal lattice was introduced by the inclusion of a structure-directing CN···S interaction (as observed in several cyano-functionalised dithiadiazolyl radicals described earlier) [24]. However the relative displacements of these supramolecular chains precluded any close intermolecular contacts between heterocyclic rings. Indeed the closest of these was beyond 6 Å. Unsurprisingly, on the basis of the direct exchange mechanism proposed here, radical **7** was found to behave as a perfect Curie paramagnet ($|\theta| < 1$ K) [24].

The dithiadiazolyl ring system is only one of a number of thiazyl-based radicals. The success of these results to rationalize the magnetic behaviour of dithiadiazolyl radicals, augers well for the extension of this methodology to other related ring systems, such as the dithiazolyls [43] **8** and thiadiazenes **9** [44]. Initial studies [45] on the trithiatriazapentalenyl radical, **10** have indicated that this approach may be applied with success to other thiazyl ring systems.

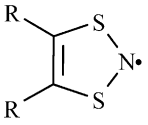

8

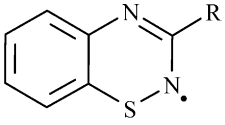

9

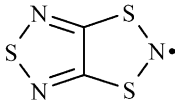

10

4. Conclusion

An ab initio DFT analysis of the exchange interactions in a series of dithiadiazolyl radicals, coupled with a SOMO–SOMO analysis of the magnetic orbitals, indicates that the exchange interaction can be considered to arise out of a direct exchange process. The DFT calculations of the exchange interaction energy, ***J***, appear to provide a reliable estimate of both the sign and magnitude of the exchange interaction.

5. Experimental

The calculation of the exchange interactions between nearest neighbour molecules was undertaken using the broken symmetry approach [15]; The broken symmetry state is a DFT state composed of pure magnetic states with different spin symmetries in such a way that all the α magnetic orbitals are located on one magnetic centre and all the β-orbitals are located on the second magnetic centre. The strength of the exchange interaction is then determined using the scheme proposed by Yamaguchi [16] using the expectation values for the high spin and low spin states:

$$\boldsymbol{J} = \frac{-(E_{\mathrm{HS}} - E_{\mathrm{BS}})}{\langle S^2\rangle_{\mathrm{HS}} - \langle S^2\rangle_{\mathrm{LS}}} \quad (4)$$

In all cases atomic coordinates for pairs of neighbouring molecules were taken from the published crystallographic data [18,23,29,33].

Acknowledgements

We would like to thank the C.I.C.Y.T. (grant MAT2001-3507-C02-02) for financial support. We are also extremely grateful to the referees for their constructive criticism of this manuscript.

References

[1] M. Tamura, Y. Nakazawa, D. Shiomi, K. Nozawa, Y. Hosokoshi, M. Ishikawa, M. Takahashi, M. Kinoshita, Chem. Phys. Lett. 186 (1991) 401;
R. Chiarelli, M.A. Novak, A. Rassat, J.L. Tholence, Nature 363 (1993) 147;
P.M. Allemand, K.C. Khemani, A. Koch, F. Wudl, K. Holczer, S. Donovan, G. Gruner, J.D. Thompson, Science 253 (1991) 301.
[2] J.M. Rawson, A. Alberola, Molecules 9 (2004) 713.
[3] E. Coronado, R. Georges, B.S. Tsukerblat, in: E. Coronado, P. Delhaes, D. Gatteschi, J.S. Miller (Eds.), Molecular Magnetism: From Molecular Assemblies to the Devices, NATO-ASI Series, E 321, p. 65.
[4] J. Goodenough, Phys. Rev. 100 (1955) 564;
J. Kanamori, J. Phys. Chem. Sol. 10 (1959) 87;
P.W. Anderson, Phys. Rev. 115 (1959) 2.
[5] H.M. McConnell, J. Chem. Phys. 39 (1963) 1910.
[6] A. Izoka, S. Murata, T. Sugawara, H. Iwamura, J. Am. Chem. Soc. 107 (1985) 1786.
[7] J.J. Novoa, M. Deumal, Struct. Bonding 100 (2001) 33.
[8] For reviews on the prediction of crystal structure and use of supramolecular synthons see: A. Gavezzotti, Cryst. Rev. 7 (1998) 5;
A. Gavezzotti, Acc. Chem. Res. 27 (1994) 309;
G.R. Desiraju, Angew. Chem. Int. Ed. Engl. 34 (1995) 2311;
J.J. Novoa, in: J.A.K. Howard, F.H. Allen, G.P. Shileds (Eds.), Implications of Molecular and Materials Structure for New Technologies, Kluwer Academic Publishers, Dordrecht, 1999;
G. Desiraju, Crystal Engineering: The Design of Organic Solids, Elsevier, Amsterdam, 1989.
[9] S.V. Kolotuchin, P.A. Thiessen, E.E. Fenlan, S.R. Wilson, C.J. Loweth, S.C. Zimmerman, Chem. Eur. J. 5 (1999) 2537;
J.M.A. Robinson, D. Philp, K.D.M. Harris, B.M. Karinki, New. J. Chem. 24 (2000) 799;
K. Biradha, Cryst. Eng. Commun. 5 (2003) 374.
[10] For recent studies on crystal structure prediction see: J.P.M. Lommersee, S.D.W. Motherwell, H.L. Ammon, J.D. Dunitz, A.

Gavezzotti, D. Hofmann, F.J.J. Leusen, W.T.M. Mooij, S.L. Price, B. Schweitzer, M.U. Schmidt, B.P. van Eijck, P. Verwer, D.E. Williams, Acta Crystallogr. B56 (2000) 697;
S.D.W. Motherwell, H.L. Ammon, J.D. Dunitz, A. Dzyabchenko, P. Erk, A. Gavezzotti, D.W.M. Hofman, F.J.J. Leusen, J.P.M. Lommersee, W.T.M. Mooij, S.L. Price, H. Scherage, B. Schweitzer, M.U. Schmidt, B.P. van Eijk, P. Verwer, D.E. Williams, Acta Crystallogr. B58 (2002) 647.
[11] J.M. Rawson, F. Palacio, Struct. Bonding 100 (2001) 93.
[12] A.D. Bond, D.A. Haynes, C.M. Pask, J.M. Rawson, J. Chem. Soc., Dalton Trans. (2002) 2522.
[13] See for example: W.T. Borden, Rev. Comp. Chem. 13 (1999) 1.
[14] M. Deumal, J. Ribas-Arino, M.A. Robb, J. Ribas, J.J. Novoa, Molecules 9 (2004) 757.
[15] L. Noodleman, J.G. Norman, J. Chem. Phys. 70 (1979) 4903;
L. Noodleman, J. Chem. Phys. 74 (1981) 5737.
[16] H. Nagao, M. Nishino, Y. Shigeta, T. Soda, Y. Kitagawa, T. Onishi, Y. Yoshioka, K. Yamaguchi, Coord. Chem. Rev. 198 (2000) 265.
[17] E. Ruiz, J. Cano, S. Alvarez, P. Alemany, J. Comp. Chem. 20 (1999) 1391.
[18] A.J. Banister, N. Bricklebank, I. Lavender, J.M. Rawson, C.I. Gregory, B.K. Tanner, W. Clegg, M.R.J. Elsegood, F. Palacio, Angew. Chem. Int. Ed. Engl. 35 (1996) 2533.
[19] F. Palacio, G. Antorrena, M. Castro, R. Burriel, J.M. Rawson, J.N.B. Smith, N. Bricklebank, J. Novoa, C. Ritter, Phys. Rev. Lett. 79 (1997) 2336.
[20] F.L. Pratt, A.E. Goeta, F. Palacio, J.M. Rawson, J.N.B. Smith, Physica B289 (2000) 119;
J.M. Rawson, A. Alberola, H. El-Mkami, G.M. Smith, J. Phys. Chem. Sol. 65 (2004) 727;
A. Alberola, C.M. Pask, J.M. Rawson, E.J.L. McInnes, J. Wolowska, H. El-Mkami, G.M. Smith, J. Phys. Chem. B 107 (2003) 14158.
[21] M. Mito, T. Kawae, K. Takeda, S. Takagi, Y. Matsushita, H. Deguchi, J.M. Rawson, F. Palacio, Polyhedron 20 (2001) 1509.
[22] P.J. Langley, J.M. Rawson, J.N.B. Smith, M. Schuler, R. Bachmann, A. Schweiger, F. Palacio, G. Antorrena, G. Gescheidt, A. Quintel, P. Rechsteiner, J. Hulliger, J. Mater. Chem. 9 (1999) 1431.
[23] A.J. Banister, N. Bricklebank, W. Clegg, M.R.J. Elsegood, C.I. Gregory, I. Lavender, J.M. Rawson, B.K. Tanner, J. Chem. Soc., Chem. Commun. (1995) 679.
[24] A. Alberola, R.J. Less, F. Palacio, C.M. Pask, J.M. Rawson, Molecules 9 (2004) 771.
[25] G. Antorrena, S. Brownridge, T.S. Cameron, F. Palacio, S. Parsons, J. Passmore, L.K. Thompson, F. Zarlaida, Can. J. Chem. 80 (2002) 1568.
[26] A.W. Cordes, R.C. Haddon, R.G. Hicks, R.T. Oakley, T.T.M. Palstra, Inorg. Chem. (1992) 1802;
A.W. Cordes, C.M. Chamchoumis, R.G. Hicks, R.T. Oakley, K.M. Yound, R.C. Haddon, Can. J. Chem. (1992) 919.
[27] J.E. Greedan, J. Mater. Chem. 11 (2001) 37.
[28] F. Palacio, in: F. Placio, E. Ressouche, J. Schweizer (Eds.), Introduction to Physical Techniques in Molecular Magnetism: Structural and Macroscopic Techniques, Publ. Universidad de Zaragoza, 2001.
[29] A. Alberola, R.J. Less, C.M. Pask, J.M. Rawson, F. Palacio, P. Oliete, C. Paulsen, A. Yamaguchi, D.M. Murphy, R.D. Farley, Angew. Chem. Int. Ed. Engl. 42 (2003) 4782.
[30] Y. Yoshida, Y. Inagaki, T. Kawae, K. Takeda, M. Mito, F. Palacio, J.M. Rawson, Presented at the International Conference on Molecular Magnetism, Tsukuba, Japan, 2004, Unpublished results.
[31] A.J. Banister, J.M. Rawson, I. Lavender, N. Bricklebank, C.I. Gregory, B.K. Tanner, Unpublished results.
[32] N. Bricklebank, S. Hargreaves, S. Spey, Polyhedron 19 (2000) 1163; See also T.M. Barclay, A.W. Cordes, N.A. George, R.C. Haddon, M.E. Itkis, R.T. Oakley, Chem. Commun. (1999) 2269.
[33] G. Antorrena, J.E. Davies, M. Hartley, F. Palacio, J.M. Rawson, J.N.B. Smith, A. Steiner, Chem. Commun. (1999) 1393.
[34] H.-U. Hofs, J.W. Bats, R. Gleiter, G. Hartmann, R. Mews, M. Eckert-Maksic, H. Oberhammer, G.M. Sheldrick, Chem. Ber. 118 (1985) 3781;
A.W. Cordes, C.D. Bryan, W.M. Davis, R.H. de Laat, S.H. Glarum, J.D. Goddard, R.C. Haddon, R.G. Hicks, D.K. Kennepohl, R.T. Oakley, S.R. Scott, N.P.C. Westwood, J. Am. Chem. Soc. 115 (1993) 7232.
[35] C.M. Aherne, A.J. Banister, I.B. Gorrell, M.I. Hansford, Z.V. Hauptman, A.W. Luke, J.M. Rawson, J. Chem. Soc., Dalton Trans. (1993) 967.
[36] J.M. Rawson, A.J. Banister, I. Lavender, Adv. Heterocycl. Chem. 62 (1995) 137, and references therein.
[37] J.M. Rawson, A.J. Banister, I. May, Magn. Reson. Chem. 32 (1994) 487.
[38] J. Luzon, J. Campo, F. Palacio, G.J. McIntyre, A.E. Goeta, E. Ressouche, C.M. Pask, J.M. Rawson, Physica B 335 (2003) 1.
[39] R.E. Del Sesto, R.D. Sommer, J.S. Miller, Cryst. Eng. Commun. 47 (2001) 1.
[40] W.V.F. Brooks, N. Burford, J. Passmore, M.J. Schriver, L.H. Sutcliffe, J. Chem Soc., Chem. Commun. (1987) 69;
E.G. Awere, N. Burford, C. Mailer, J. Passmore, M.J. Schriver, P.S. White, A.J. Banister, H. Oberhammer, L.H. Sutcliffe, J. Chem. Soc., Chem. Commun. (1987) 66;
S.A. Fairhurst, K.M. Johnson, L.H. Sutcliffe, K.F. Preston, A.J. Banister, Z.V. Hauptman, J. Passmore, J. Chem. Soc., Dalton Trans. (1986) 1465.
[41] S.C. Nyburg, C.H. Faerman, Acta Crystallogr. 41 (1985) 274.
[42] G. Filippini, A. Gavezzotti, J.J. Novoa, Acta Crystallogr. B 55 (1999) 543.
[43] See for example G.D. McManus, J.M. Rawson, Coord. Chem. Rev. 189 (1999) 135;
J.M. Rawson, F. Palacio, Struct. Bonding 100 (2001) 93, and references therein.
[44] P. Kaszynski, Molecules 9 (2004) 716.
[45] W. Fujita, K. Awaga, Science 286 (1999) 281;
G.D. McManus, J.M. Rawson, N. Feeder, E.J.L. McInnes, J.J. Novoa, R. Burriel, F. Palacio, P. Oliete, J. Mater. Chem. 11 (2001) 1992.